Scientific Research Publishing

International Journal of Geosciences, 2023, 14, 238-250
https://www.scirp.org/journal/ijg
ISSN Online: 2156-8367
ISSN Print: 2156-8359

Relative Dielectric Permittivity Variations during Compaction as a Mean of Compaction Quality Control: Case Study on Laterite Samples from Senegal

Mapathé Ndiaye, Makhaly Ba, Teophile Kiendrebeogo, Linda E. Gaffo Foudjo

Laboratoire de Mécanique et de Modélisation, Université de Thiès, Sénégal
Email: mapathe.ndiaye@univ-thies.sn

How to cite this paper: Ndiaye, M., Ba, M., Kiendrebeogo, T. and Foudjo, L.E.G. (2023) Relative Dielectric Permittivity Variations during Compaction as a Mean of Compaction Quality Control: Case Study on Laterite Samples from Senegal. *International Journal of Geosciences*, **14**, 238-250.
https://doi.org/10.4236/ijg.2023.142012

Received: January 4, 2023
Accepted: February 14, 2023
Published: February 17, 2023

Abstract

This study explores an alternative to the classical use of direct methods, as water content and dry density measurements, for compaction quality control. For this purpose, the dielectric properties of lateritic materials are determined by radar method and are compared with the permittivity determined from the Topp formula and from the CRIM model. This approach allowed to establish a relationship between the geotechnical properties determined during compaction such as dry density, water content or porosity with dielectric permittivity. The obtained results made it possible to determine an optimum dielectric permittivity corresponding to the optimum dry density and the optimum water content that could be used for non-destructive *in situ* compaction testing. Such an approach should improve the implementation and effectiveness of *in situ* compaction quality control of geotechnical infrastructures.

Keywords

Laterite, Proctor, Water Content, Dry Density, Dielectric Permittivity

1. Introduction

The context of rarefaction of high-quality building materials and the concern to reduce the costs of geotechnical infrastructure are constraints on the critical distances of search for laterites used as borrow materials in Senegal [1]. As a result, materials available within the optimum radius for use in road, dyke or embankment construction may require stabilization or improvement [2]. Compaction to improve their mechanical properties is almost always necessary [3]. To ensure

proper *in situ* implementation and to check compliance between parameters determined from laboratory measurements and on-site implementation, compaction parameters must be controlled using different quality control procedures. There are several approaches to measuring *in situ* compaction. The available methods include the sand cone test, the membrane densitometer test or the gamma densimeter [4]. However, most common methods, such as the membrane densitometer, the compacted sand method, in addition to being tedious to implement, use an invasive and destructive process. Another major difficulty rises from the spatial limitation of the obtained results, which do not allow to account for heterogeneity in the implementation of materials [5]. The difficulties and limitations encountered in the use of direct methods for *in situ* compaction quality control have motivated our investigations of the possibility of using indirect methods, such as the geophysical radar method in compaction quality control. The radar provides information on the dielectric properties of materials [6].

Several studies have established relationships between dielectric and geotechnical properties ([7]-[12]). Also, unlike *in situ* compaction assessment direct methods, the dielectric properties of materials are easy and quick to determine ([13] [14] [15]). As a result, the measurement of *in situ* dielectric properties should make it possible to deduce compaction parameters in order to facilitate and optimize quality control.

The purpose of this study is to search, in the context of laterite materials commonly used in construction, to determine the existing relationship between the dielectric properties measured by radar method and the electrical properties calculated from the compaction parameters. Establishing such a relationship is of high importance to improve the implementation and effectiveness of *in situ* compaction quality control of geotechnical infrastructures.

2. Material and Method

On laterite soil samples from the quarry of Diack, in the region of Thies in Senegal, we studied the variation of dry density ρ_d as a function of the mass water content w. To proceed, the material is compacted at different water contents, in accordance with the modified Proctor test NF P 94-093 [16].

First, the mass water content w is determined by the relation:

$$w = \frac{m_h - m_s}{m_s} \tag{1}$$

With m_h the mass of the wet sample and m_s the mass of the dried sample.

The dried density ρ_d is determined, taking into account the actual volume of the used mold with the relation:

$$\rho_d = \frac{\rho_h}{100 + w} * 100 \tag{2}$$

with ρ_h the wet density of the sample.

$\rho_h = \frac{\gamma_h}{\gamma_w}$ with γ_h the specific density of the wet material γ_h and $\gamma_w \approx 1\,\mathrm{g/cm^3}$, the specific density of water.

The volumetric water content θ is given by the relation:

$$\theta = \frac{\rho_d}{\rho_w} w$$

with ρ_d the dried density of the sample, ρ_w the specific density of water et w the mass water content.

At each stage of compaction, the porosity ϕ of the material is determined by the relation:

$$\phi = 1 - \frac{\rho_d}{\rho_s}$$

At the same time, at each stage of compaction, with a given water content and dried density, the dielectric permittivity was measured using the Ground Penetrating Radar (GPR) method or Radar [17].

The principle of GPR is based on the emission and reception of electromagnetic waves passing through the investigated material. Waves are sent as impulses in the time domain [18].

The propagation of radar waves in a medium depends on the dielectric properties, and more on the permittivity of the material. The velocity v of radar waves through a medium is given by the relation:

$$v = \frac{c}{\sqrt{\varepsilon_r}} \tag{3}$$

With $c = 0.3\,\mathrm{m/ns}$ corresponding to the radar wave velocity through the air. ε_r is the relative permittivity of the material and corresponds to the ratio of effective permittivity ε_e and air permittivity ε_0 taken as reference.

The device used for permittivity measurements by radar method includes a GSSI SIR 3000 acquisition unit connected to a 1.6 GHz GSSI central frequency antenna (**Figure 1**).

Radar data acquisition for permittivity determination was carried out using a specially designed device (see **Figure 2**), facilitating the passage of the monostatic radar antenna, mounted on a cart model 319, over the compacted sample still in the mold.

The determination of the permittivity of laterite soil samples by the GPR method is based on the two-way travel time method [19]. In our case, this method consists of pointing the travel time of the radar wave, between the top and the base of the mold, clearly visible on the radar profile and marked by reflections due to the permittivity contrast between the air and the surface of the sample on the one hand, and between the base of the sample and the mold support on the other hand. From the travel time, the speed v of the radar signal is written.

Figure 1. SIR3000 radar acquisition system with 1.6 GHz antenna and accessories.

Figure 2. Data acquisition device, showing the laterite soil sample in the Proctor mold and the 1.6 GHz antenna.

$$v = \frac{2d}{t} \tag{4}$$

t is the two-way travel time, and d is the length of the wave ray inside the mold. In our conditions, $d = 12.5\,\text{cm}$.

If we pose equations 3 = 4, we can deduce the relative permittivity ε_r with the relation:

$$\varepsilon_r = \left[\frac{ct}{2d}\right]^2 \tag{5}$$

The picking of radar signal travel time inside the sample was performed on each profile under Reflex2DQuick software [20].

In order to determine the experimental dielectric properties from the compaction data for comparison with the permittivity obtained by radar measurements, we used the Topp law [9] and the Lichteneker-Rother model [7].

Topp's law is an empirical law linking volumetric water to relative permittivity ε_r. It was derived from the correlation of water content measurements and dielectric constants on various laboratory samples [9]. Topp's law states that:

$$\varepsilon_r = 3.03 + 9.3\theta + 146\theta^2 - 76.7\theta^3 \quad (6)$$

ε_r is the relative permittivity and θ is the volumetric water content.

Topp's law is valid for frequencies ranging from 10 MHz to 1 GHz and water contents from 5% to 17% [21]. However, it is inappropriate for clayey and organic matter rich soils. At higher frequencies and near-water saturation (40%), Topp's law may overestimate relative permittivity [22].

Other authors ([10] [23]) have suggested empirical relationships that also allow volumetric water content to be recovered from relative permittivity. They are expressed as follows:

$$\theta = 0.00701 + 0.0347\varepsilon_r - 11.6\times10^{-4}\varepsilon_r^2 + 18\times10^{-6}\varepsilon_r^3 \quad (7)$$

$$\theta = -0.0725 + 0.0367\varepsilon_r - 12.3\times10^{-4}\varepsilon_r^2 + 15\times10^{-6}\varepsilon_r^3 \quad (8)$$

The Lichteneker-Rother model also referred to as Complex Refractive Index Model—CRIM [7] is a volumetric model in which the material is considered as a medium consisting essentially of solid grains of the same nature, voids and water. The CRIM model is valid for medium with low salinity and low dielectric loss. It allows to connect the permittivity to the porosity and the water content by the relation:

$$\sqrt{\varepsilon_r} = \theta\sqrt{\varepsilon_w} + (\phi - \theta) + (1-\phi)\sqrt{\varepsilon_s} \quad (9)$$

θ is volumetric water content $\theta = \frac{\rho_d}{\rho_w} w$ and ϕ is the porosity. We consider the relative permittivity of water $\varepsilon_w = 80.1$.

As stated by Knoll [24] and Robinson *et al.*, [25], we can assume for the solid particles fraction of the sample a permittivity $\varepsilon_s \approx 5$

The main steps of the approach used in this study, including the compaction of the laterite soil material, the determination of the compaction parameters, the determination of the relative permittivity using both empirical and physical laws and by the radar method, are summarized in the diagram below (**Figure 3**).

3. Results and Discussion

The compaction parameters, determined during the modified Proctor test, namely the mass water content *w*, the wet density ρ_h, the dried density ρ_d, the volumetric water content θ and the porosity ϕ, are shown in the table below (**Table 1**).

The Proctor curve, corresponding to the variation of the dried density as a function of the mass water content, is shown in **Figure 4** below.

The Proctor curve (**Figure 4**) shows that the optimum water content w_{OPM} and the optimum dried density γ_{dOPM} are respectively 16.8% and 1.83 g/cm^3.

Figure 5 shows the radar facies corresponding to the tested sample and the

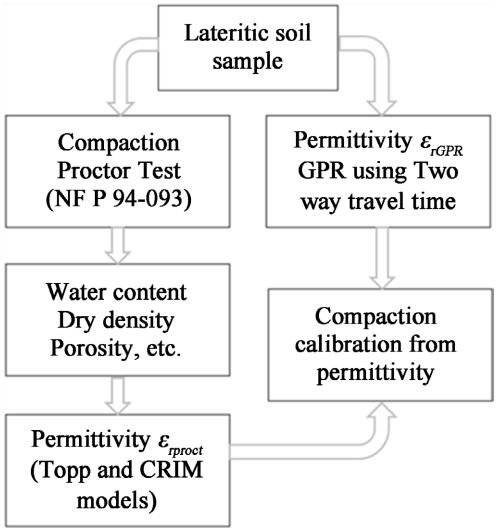

Figure 3. Flow diagram of the steps of the experimental approach of this study.

Table 1. Evolution of compaction parameters during the modified Proctor test.

w (%)	ρ_h (g/cm^3)	ρ_d (g/cm^3)	θ	ϕ
14.71	2.04	1.78	0.262	0.321
16.25	2.10	1.80	0.292	0.313
16.97	2.14	1.83	0.310	0.301
19.3	2.11	1.77	0.342	0.324

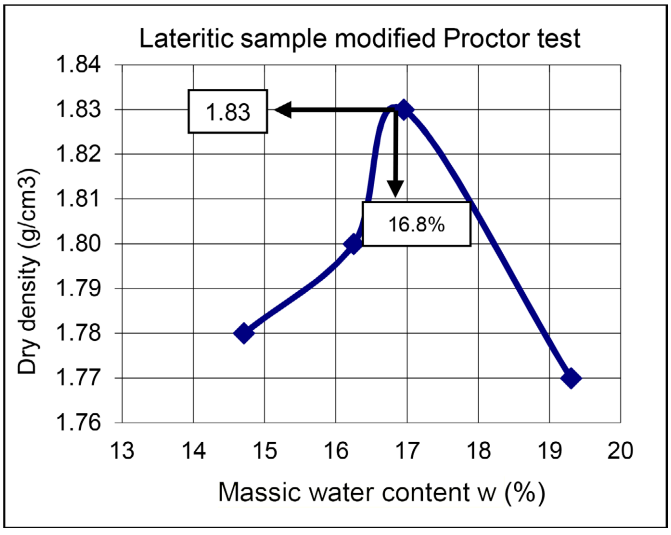

Figure 4. Proctor curve of the laterite soil sample.

limits of the mold. In the following steps, only the part of the profile around the mold is shown. The radar profiles obtained at each stage of compaction for each water content and corresponding dried density are shown in **Figure 6**.

The dielectric permittivity's determined from the Topp law, the CRIM model and the radar method are summarized in the table below (**Table 2**).

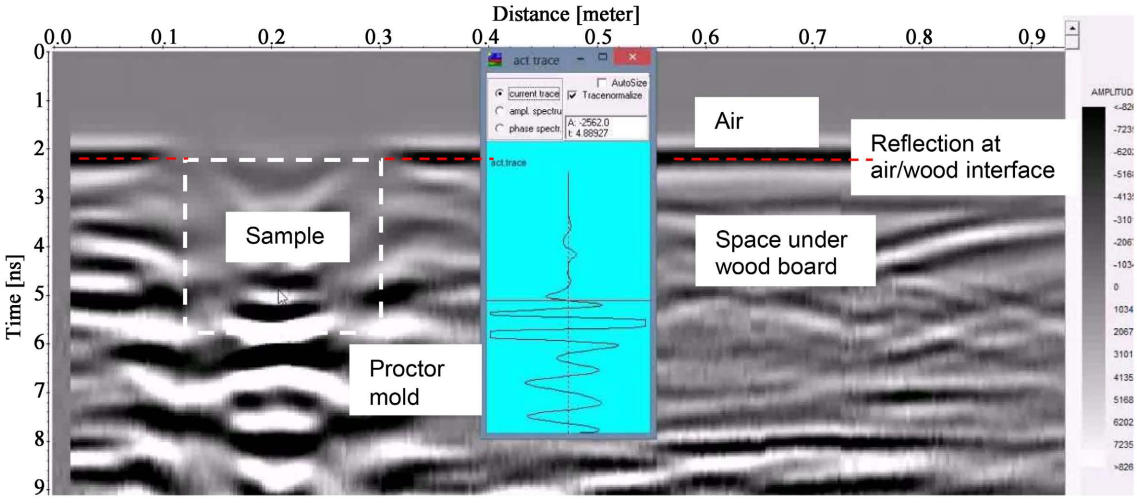

Figure 5. Overview of a radar profile showing the radar facies corresponding to the tested sample and the limits of the mold (see annotations).

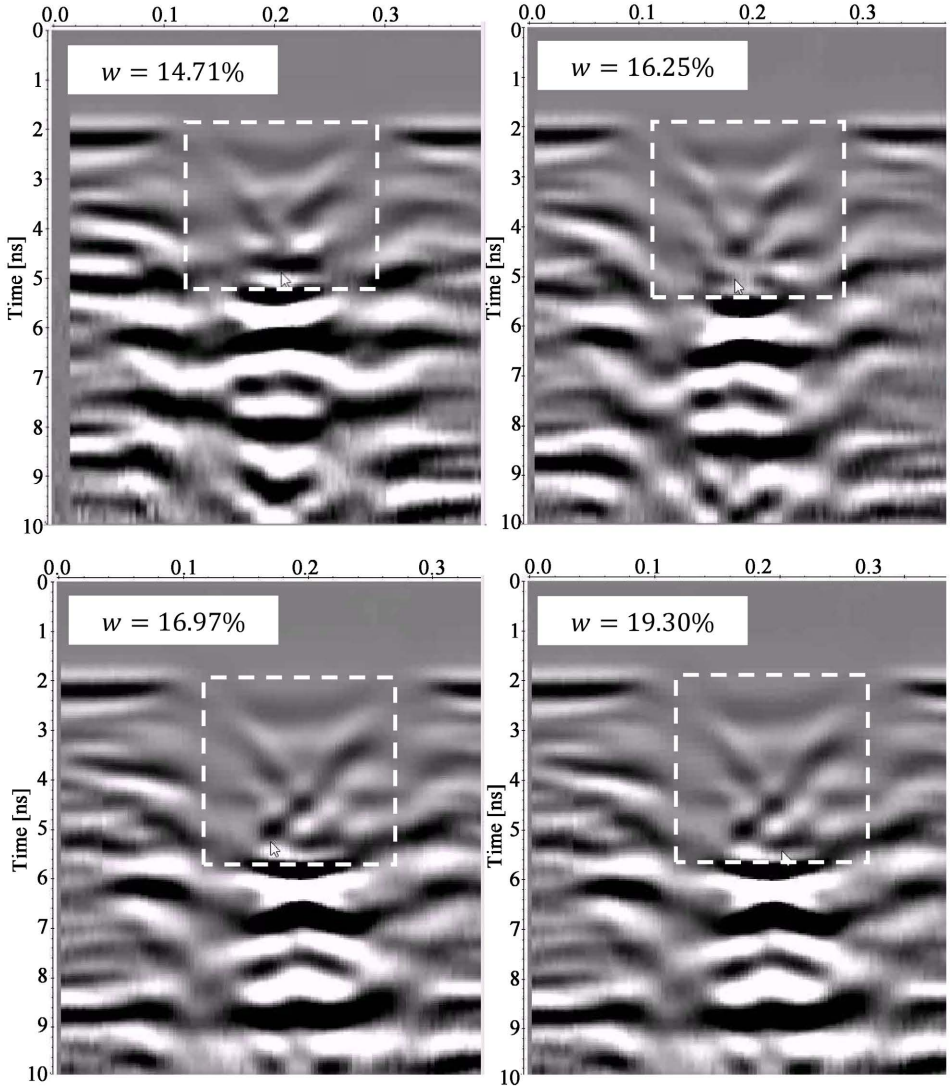

Figure 6. Radar profiles obtained at the various stages of the compaction.

Table 2. Summary of the obtained relative dielectric permittivity (dimensionless). ε_{rT} is the permittivity from Topp law, ε_{rC} is the permittivity from CRIM law and ε_{rGPR} is the permittivity determined from radar method.

w (%)	14.71	16.25	16.97	19.3
ρ_h (g/cm^3)	2.04	2.1	2.14	2.11
ρ_d (g/cm^3)	1.78	1.8	1.83	1.77
θ	0.262	0.292	0.31	0.342
ϕ	0.321	0.313	0.301	0.324
ε_{rT}	14.10	16.32	17.70	20.18
ε_{rC}	15.37	17.43	18.77	20.71
ε_{rGPR}	10.42	11.86	13.39	14.84

Several correlations were performed to understand the relationship between the various parameters determined during compaction (**Table 1**) and the obtained relative permittivity (**Table 2**).

In a first step, we correlated the density and mass water contents with the different permittivities (**Figure 7**). In a second step, wet and dried densities were correlated with permittivities (**Figure 8**). Finally, the porosity is correlated with the permittivities (**Figure 9**).

The correlation between permittivity and water content (**Figure 7**) shows that the permittivity of the sample increases linearly with the water content. This increase is valid for all three types of permittivity. The correlation coefficients are between 95% and 97% for the mass water content, and between 98% and 99% for the volumetric water content with a 99% confidence interval verified for a number of samples $n = 4$.

The linearity of the relation can be explained by the fact that, when the water content increases, the air previously contained in the voids of the material is gradually replaced by water. Thus, the permittivity of the material evolves towards the permittivity of the water which corresponds to the maximum permittivity ($\varepsilon_{r_{eau}} > 80$). Moreover, in the presence of water, the polarization capacity of the medium increases due to the polarity of the water molecules, resulting in dielectric loss [26]. The better correlation with the volumetric water content compared to the mass water content is due to the fact that, the mass water content only takes into account the free water that can be removed by drying in the oven [27].

The correlation of permittivity with density (**Figure 8**) gives a bell-shaped curve. At low relative permittivity, the density increases with the permittivity until we reach the optimal density γ_{OPM}. Beyond, the density decreases with the permittivity. This curve allows us to determine the permittivity at the optimum which is respectively 13.39, 17.77 et 18.77 for $\varepsilon_{rOPM\,GPR}$, $\varepsilon_{rOPM\,Topp}$ and $\varepsilon_{rOPM\,CRIM}$.

Even if the optimum permittivity varies according to the method of determination, the shape of the curve remains substantially the same, with a left or right

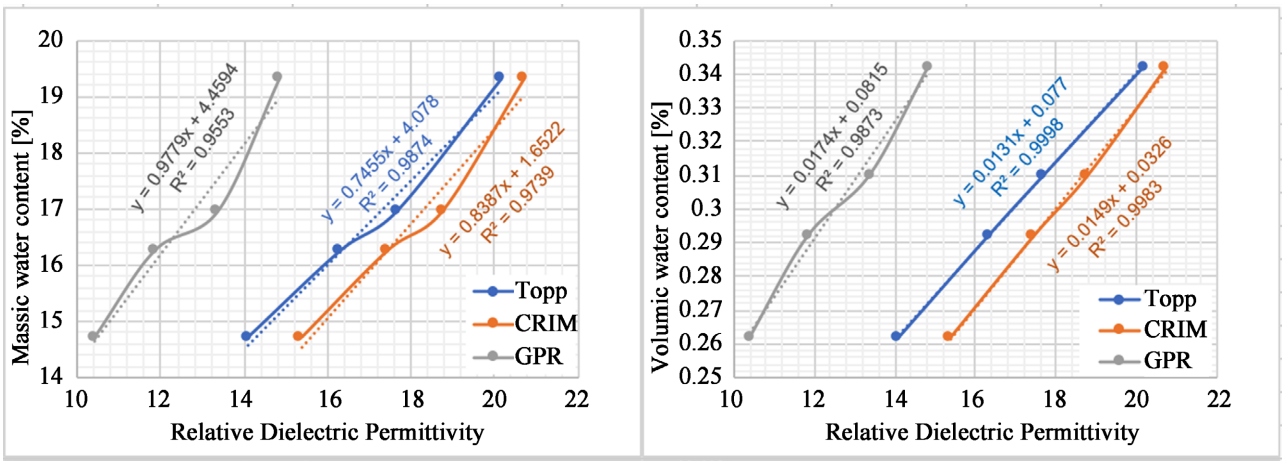

Figure 7. Correlation between the permittivity obtained by different methods (Topp formula, CRIM model and GPR) with the mass water content and volumetric water content.

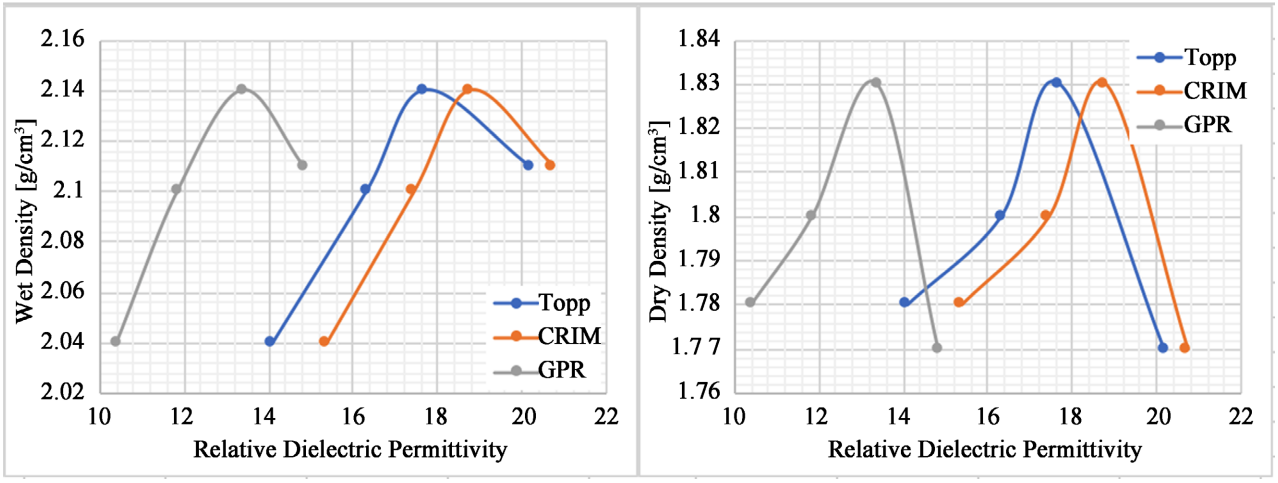

Figure 8. Correlation between the permittivity obtained by different methods (Topp formula, CRIM model and GPR) with the wet density and the dried density.

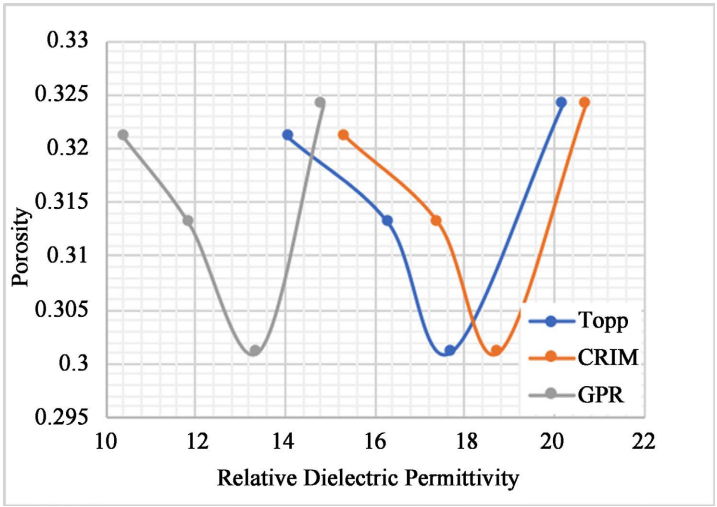

Figure 9. Correlation between the permittivity obtained by different methods (Topp formula, CRIM model and GPR) with the porosity.

offset. Also, the shape of the permittivity/density curve, identical to that of the Proctor curve (dry density as a function of mass water content) means that, like the water content, permittivity could indeed serve as an indicator of compaction. This is substantiated by the linear correlation between permittivity and water content (see **Figure 7**).

The correlation of the porosity with the permittivity (**Figure 9**) shows an inverted bell-shaped curve, with a minimal porosity corresponding to the optimal permittivity. The decrease in porosity at the optimum is related to grain tightening. Beyond the optimum, the increase in porosity can be explained by the cracking and breaking of grains related to compaction energy ([28] [29]).

The various correlations show that, even if the value of the permittivity varies from one determination method to another, the shape of the curve remains unchanged. The maximum permittivities are obtained with the CRIM model, followed by the Topp law and the GPR method.

These differences in permittivity are explained by the fact that, these different methods evaluate permittivity by focusing on different parameters. The very high values observed with the CRIM model could be explained by the fact that this model considers the sample as a composite material with a solid fraction consisting of the grains, a liquid fraction consisting of water and a gaseous fraction filling the voids of the medium. It considers that the solid phase consists of grains of the same mineralogic nature, which is not the case for laterite. Indeed, many studies have shown that, apart from the iron oxide rich gravelly, laterite may contain a more or less large clay fraction or other weathering minerals or parent rock residues [30].

The permittivity obtained from Topp model could have been influenced by the frequency of the antenna, which is 1.6 GHz while the model was established from measurements with a frequency band of 10 MHz to 1 GHz. This confirms the decrease in permittivity with the decreasing frequency suggested by several authors ([31] [32] [33]). In addition, the metallic walls of the Proctor mold may cause interference due to the total reflection of radar waves on metallic objects [34].

Nevertheless, despite the lower permittivities obtained by GPR measurements compared to the those obtained from the Topp formula and the CRIM model, the similar shape of the curves ensures the reproducibility of the permittivity/compaction properties relation. In addition, the curves show that the optimal permittivity can be used to identify the optimum dry density, corresponding to an optimum water content and an optimum porosity.

By regression, it is possible to establish the law linking the permeability, measured by GPR method to the dry density.

The relationship between permittivity and dry density is expressed as:

$$\rho_d = -0.0051\varepsilon_r^3 + 0.1826\varepsilon_r^2 - 2.1663\varepsilon_r + 10.256$$

4. Conclusions

The study of the relationship between the dielectric permittivity according to the

Topp formula, the CRIM model and the geophysical radar method made it possible to understand its relationship with the compaction parameters. Due to the good correlation between water content and permittivity, the trend of the compaction curve can be reproduced by the curve of the dry density variation as a function of the permittivity, which makes it possible to determine a permittivity at the optimum Proctor.

Even if the value of the permittivity changes depending on the method of determination, the fact remains that, for the different methods, it remains possible to determine the optimal permittivity linked to the optimal density.

The resemblance of the gaits allows seeing the correspondence between the permittivity and the optimal dry density used in the quality control of compaction.

During the *in-situ* quality control of compaction, investigations using radar method should make it possible to evaluate the optimal permittivity as a proxy for monitoring the optimal compaction.

In order to generalize the use of this procedure in the compaction quality control, it should be necessary to carry out a parametric study on various laterite samples at various frequencies with various water content. It should also be necessary to tighten the water content steps to improve the accuracy on the Proctor curve and its equivalence with the Proctor curve from GPR method.

Conflicts of Interest

The authors declare no conflicts of interest regarding the publication of this paper.

References

[1] Samb, F., Fall, M., Berthaud, Y. and Ba, M. (2013) Resilient Modulus of Compacted Lateritic Soils from Senegal at OPM Conditions. *Geomaterials*, **3**, 165-171. https://doi.org/10.4236/gm.2013.34021

[2] Ogunsanwo, O. (1989) Some Geotechnical Properties of Two Laterite Soils Compacted at Different Energies. *Engineering Geology*, **26**, 261-269. https://doi.org/10.1016/0013-7952(89)90013-6

[3] Fall, M., Tisot, J.P. and Cissé, I.K. (1995) Comportement mécanique à l'appareil de cisaillement de Casagrande de trois graveleux latéritiques compactés provenant du Sénégal Occidental. *Bulletin of the International Association of Engineering Geology*, **52**, 59-73. https://doi.org/10.1007/BF02602682

[4] Head, K.H. (1992) Manual of Soil Laboratory Testing. Volume 1. Soil Classification and Compaction Tests.

[5] Liu, D., Sun, J., Zhong, D. and Song, L. (2012) Compaction Quality Control of Earth-Rock Dam Construction Using Real-Time Field Operation Data. *Journal of Construction Engineering and Management*, **138**, 1085-1094. https://doi.org/10.1061/(ASCE)CO.1943-7862.0000510

[6] Busch, S., van der Kruk, J., Bikowski, J. and Vereecken, H. (2012) Quantitative Conductivity and Permittivity Estimation Using Full-Waveform Inversion of On-Ground GPR Data. *Geophysics*, *77*, H79-H91. https://doi.org/10.1190/geo2012-0045.1

[7] Lichtenecker, K.V. (1931) Die Herleitung des logarithmischen Mischungsgesetzes aus allgemeinen Prinzipien der stationaren Stromung. *Physikalische Zeitschrift*, **32**, 255-260.

[8] Archie, G.E. (1942) The Electrical Resistivity Log as an Aid in Determining Some Reservoir Characteristics. *Transactions of the AIME*, **146**, 54-62. https://doi.org/10.2118/942054-G

[9] Topp, G.C., Davis, J.L. and Annan, A.P. (1980) Electromagnetic Determination of Soil Water Content: Measurements in Coaxial Transmission Lines. *Water Resources Research*, **16**, 574-582. https://doi.org/10.1029/WR016i003p00574

[10] Jacobsen, O.H. and Schjønning, P. (1993) A Laboratory Calibration of Time Domain Reflectometry for Soil Water Measurement Including Effects of Bulk Density and Texture. *Journal of Hydrology*, **151**, 147-157. https://doi.org/10.1016/0022-1694(93)90233-Y

[11] Noborio, K. (2001) Measurement of Soil Water Content and Electrical Conductivity by Time Domain Reflectometry: A Review. *Computers and Electronics in Agriculture*, **31**, 213-237. https://doi.org/10.1016/S0168-1699(00)00184-8

[12] Thring, L.M., Boddice, D., Metje, N., Curioni, G., Chapman, D.N. and Pring, L. (2014) Factors Affecting Soil Permittivity and Proposals to Obtain Gravimetric Water Content from Time Domain Reflectometry Measurements. *Canadian Geotechnical Journal*, **51**, 1303-1317. https://doi.org/10.1139/cgj-2013-0313

[13] Wang, J.R. and Schmugge, T.J. (1980) An Empirical Model for the Complex Dielectric Permittivity of Soils as a Function of Water Content. *IEEE Transactions on Geoscience and Remote Sensing*, **GE-18**, 288-295. https://doi.org/10.1109/TGRS.1980.350304

[14] Bradford, J.H., Harper, J.T. and Brown, J. (2009) Complex Dielectric Permittivity Measurements from Ground-Penetrating Radar Data to Estimate Snow Liquid Water Content in the Pendular Regime. *Water Resources Research*, **45**. https://doi.org/10.1029/2008WR007341

[15] Knyazev, N.S. and Malkin, A.I. (2017) Dielectric Permittivity and Permeability Measurement System. *CEUR Workshop Proceedings*, Yekaterinburg, 9 December 2017, 45-51.

[16] NF P 94-093 (1999) Détermination des références de compactage d'un matériau. 21 p.

[17] BLPC n° 211 (1997) Applications du radar géologique en génie civil. 117-131.

[18] Annan, A.P. (2009) Electromagnetic Principles of Ground Penetrating Radar. In: Jol, H.M., Ed., *Ground Penetrating Radar: Theory and Applications*, Elsevier, Amsterdam, 1, 3-40. https://doi.org/10.1016/B978-0-444-53348-7.00001-6

[19] Le Bastard, C., Wang, Y., Baltazart, V. and Derobert, X. (2013) Time Delay and Permittivity Estimation by Ground-Penetrating Radar with Support Vector Regression. *IEEE Geoscience and Remote Sensing Letters*, **11**, 873-877. https://doi.org/10.1109/LGRS.2013.2280500

[20] Sandmeier, K.J. (2008) Reflex2DQuick-Program for Processing of Electromagnetic Reflection, Refraction and Transmission Data Version 1.2.1.

[21] Ercoli, M., Di Matteo, L., Pauselli, C., Mancinelli, P., Frapiccini, S., Talegalli, L. and Cannata, A. (2018) Integrated GPR and Laboratory Water Content Measures of Sandy Soils: From Laboratory to Field Scale. *Construction and Building Materials*, **159**, 734-744. https://doi.org/10.1016/j.conbuildmat.2017.11.082

[22] Van Dam, R.L. (2014) Calibration Functions for Estimating Soil Moisture from

GPR Dielectric Constant Measurements. *Communications in Soil Science and Plant Analysis*, **45**, 392-413. https://doi.org/10.1080/00103624.2013.854805

[23] Nadler, A., Dasberg, S. and Lapid, I. (1991) Time Domain Reflectometry Measurements of Water Content and Electrical Conductivity of Layered Soil Columns. *Soil Science Society of America Journal*, **55**, 938-943. https://doi.org/10.2136/sssaj1991.03615995005500040007x

[24] Knoll, M.D. (1996) A Petrophysical Basis for Ground Penetrating Radar and Very Early Time Electromagnetics: Electrical Properties of Sand-Clay Mixtures. Doctoral Dissertation, University of British Columbia, Vancouver.

[25] Robinson, D.A. and Friedman, S.P. (2003) A Method for Measuring the Solid Particle Permittivity or Electrical Conductivity of Rocks, Sediments, and Granular Materials. *Journal of Geophysical Research*: *Solid Earth*, **108**. https://doi.org/10.1029/2001JB000691

[26] Saarenketo, T. (2006) Electrical Properties of Road Materials and Subgrade Soils and the Use of Ground Penetrating Radar in Traffic Infrastructure Surveys (No. 471).

[27] Gardner, W.H. (1986) Water Content. In: Klute, A., Ed., *Methods of Soil Analysis*: *Part* 1 *Physical and Mineralogical Methods*, 5.1, The American Society of Agronomy Inc., Madison, 493-544. https://doi.org/10.2136/sssabookser5.1.2ed.c21

[28] Richard, G., Cousin, I., Sillon, J.F., Bruand, A. and Guérif, J. (2001) Effect of Compaction on the Porosity of a Silty Soil: Influence on Unsaturated Hydraulic Properties. *European Journal of Soil Science*, **52**, 49-58. https://doi.org/10.1046/j.1365-2389.2001.00357.x

[29] Fu, Y., Tian, Z., Amoozegar, A. and Heitman, J. (2019) Measuring Dynamic Changes of Soil Porosity during Compaction. *Soil and Tillage Research*, **193**, 114-121. https://doi.org/10.1016/j.still.2019.05.016

[30] Diop, B.O., Gbaguidi, I., Lo, P.G., Cisse, A., Sène, S. and Ba, M. (2021) Optimal Adaptation of the Use Conditions of Lateritic Soils in Flexible Pavements from Laboratory to the Construction Site. *Challenging Issues on Environment and Earth Science*, **4**, 78-90. https://doi.org/10.9734/bpi/ciees/v4/7919D

[31] Kelleners, T.J., Robinson, D.A., Shouse, P.J., Ayars, J.E. and Skaggs, T.H. (2005) Frequency Dependence of the Complex Permittivity and Its Impact on Dielectric Sensor Calibration in Soils. *Soil Science Society of America Journal*, **69**, 67-76. https://doi.org/10.2136/sssaj2005.0067a

[32] Kessouri, P. (2012) Mesure simultanée aux fréquences moyennes et cartographie de la permittivité diélectrique et de la conductivité électrique du sol. Doctoral Dissertation, Université Pierre et Marie Curie-Paris VI, Paris.

[33] Filali, B. (2014) Caractérisation des ondes radar de surface par la simulation numérique et les mesures GPR pour l'auscultation en génie civil. Université de Sherbrooke, Sherbrooke.

[34] Oloumi, D. and Rambabu, K. (2018) Metal-Cased Oil Well Inspection Using Near-Field UWB Radar Imaging. *IEEE Transactions on Geoscience and Remote Sensing*, **56**, 5884-5892. https://doi.org/10.1109/TGRS.2018.2827395